AN EXPERIMENTAL INVESTIGATION OF THE CAVITATIONAL CHARACTERISTICS OF CONVERGING NOZZLES

G. S. Nazarov

Inzhenerno-Fizicheskii Zhurnal, Vol. 14, No. 3, pp. 423–429, 1968

UDC 532.528

We consider problems associated with the appearance and development of cavitation in the flow of a liquid through channels with local constriction. For the case of separation flow we have derived an equation which associates the parameters of three sections of the channel: at the inlet, at the cross section of the stream, and at the outlet; this equation has been confirmed through experimentation on cold and hot water, as well as on kerosene.

Variously shaped channels made of plexiglas (Fig. 1) served as the object of the study, and each of these channels was placed inside a transparent tube connected to a container filled with a liquid whose surface was open to the atmosphere. The other end of the tube was connected to a metering container which was evacuated by means of a vacuum pump. As the liquid flowed through the channel, we determined the volumetric flow rate as a function of the pressure difference. Figure 2 shows the characteristics of six variously shaped channels—Nos. 1, 2, 3, 4, 8, and 9—with cylindrical segments of minimum cross section; in addition, there were four channels—Nos. 5, 6, 7, and 10—with minimum cross sections of various diameters and sharp edges. The curves indicate that the shape of the discharge characteristics depends on whether or not there is a cylindrical segment at the minimum cross section of the channel. In one case, the characteristics exhibit a so-called "shelf" of constant flow rate, while in another case, no such phenomenon is evident.

Visual observations revealed cavitation at the constricted portion of the channel with a drop in the outlet pressure. Initially the cavitation zone was circular; then it increased in size. With an outlet pressure close to the vapor pressure of saturated steam, flow separation occurred and a jet was formed. Flow separation occurred initially along a small segment beyond the constriction; with a further drop in the outlet pressure, the separation zone became larger, and the cavitation sheet banding the moving liquid jet spread along the tube in the direction of the flow. At the instant of complete flow separation there was a change in the sound accompanying the cavitation: instead of the characteristic crackling sound, a rustling-type sound set in.

Figure 3 shows the occurrence of separation flow. The Bernoulli equation for sections 0-0 and 1-1—neglecting losses at the channel constriction, as well as within the jet—gives us

$$c_1^2 = \frac{P_0 - P_1 + \frac{\rho}{2} c_0^2}{\frac{\rho}{2}}. \qquad (1)$$

A loss of total head occurs on sudden expansion of the jet. According to the Borda-Carnot theorem, for sections 1-1 and 2-2 we write

$$p_1^* - p_2^* = \frac{\rho}{2}(c_1 - c_2)^2,$$

where

$$p^* = p + \frac{\rho}{2} c^2.$$

Reduction of similar terms yields

$$p_1 - p_2 = \rho c_2^2 - \rho c_1 c_2,$$

whence

$$c_1 = \frac{\rho c_2^2 + (p_2 - p_1)}{\rho c_2}. \qquad (2)$$

After squaring (2) and eliminating c_1^2 from (1), we have

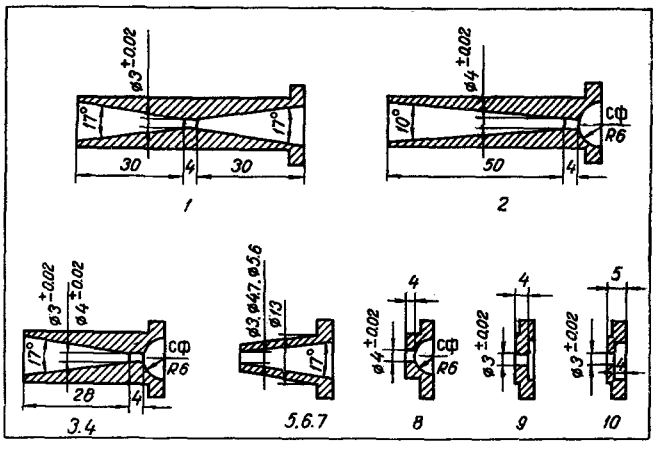

Fig. 1. Main dimensions and shape of channels Nos. 1 to 10.

$$2\rho c_2^2\left(p_0+\frac{\rho}{2}c_0^2\right)-2\rho c_2^2\left(p_2+\frac{\rho}{2}c_2^2\right)=$$

$$=(p_2-p_1)^2. \qquad (3)$$

The values of the total pressures are given in the parentheses.

This yields

$$\frac{(p_2-p_1)^2}{p_0^*-p_2^*}=4\frac{\rho}{2}c_2^2. \qquad (4)$$

Equation (4), relating the parameters of three sections of the channel—at the inlet, at a cross section of the jet, and at the outlet—characterizes the energy distribution in the liquid flow on separation.

Favorable conditions for the release of dissolved gases are established in the reduced-pressure zone by the motion of the liquid. The static pressure p_1 within the cavity is equal to the sum of the pressures $p_s + p_g$: the vapor pressure of saturated steam and the partial pressure of the gas released from the liquid. Reference [1] accordingly recommends the substitution of the sum of the pressures $p_s + p_g$ for p_s in the expression for the cavitation factor. Total separation of the flow takes place at p_2; the ratio of the excess of this latter pressure over the pressure of the vapor and the gas to the dynamic head over a broad

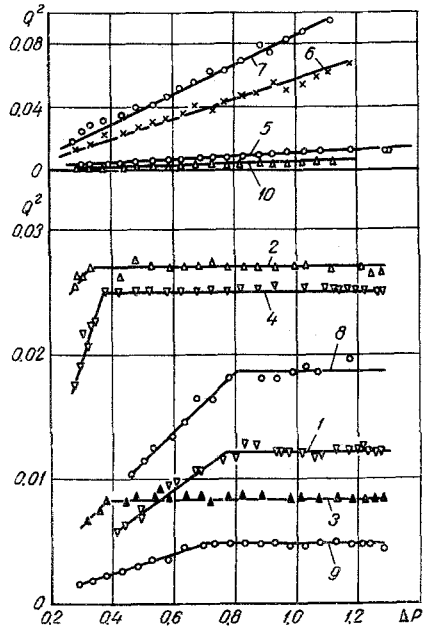

Fig. 2. Rate (l/sec) versus pressure drop (kg/cm²) for water at t = 15° C and p_0 = = 1.3 atm abs for channels of various geometry. Figures show channel numbers.

section of the channel may be regarded as the cavitation factor which determines the instant of separation:

$$\frac{p_2-(p_s+p_g)}{\frac{\rho}{2}c_2^2}=\lambda. \qquad (5)$$

We introduce a similar factor for the inlet section of the channel:

$$\frac{p_0-(p_s+p_g)}{\frac{\rho}{2}c_0^2}=K. \qquad (6)$$

Equation (4) can be presented with the aid of the dimensionless parameters K and λ for our case of equal cross-sectional areas at the inlet and outlet of

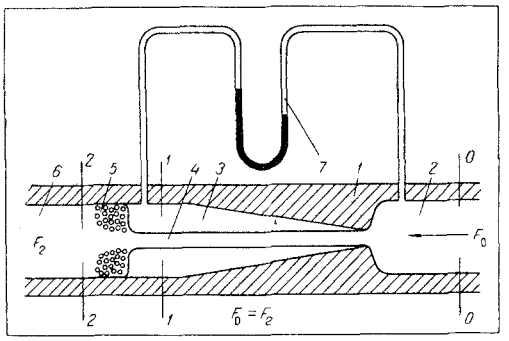

Fig. 3. Scheme of separation fluid flow: 1) working channel; 2) inlet flow; 3) steam and gas region (cavity); 4) fluid stream; 5) region of bubble cavitation; 6) outlet flow; 7) mercury differential manometer: a) it shows pressure difference p_0-p_2 at preseparation stage; b) shows pressure difference p_0-p_1 at complete flow separation. Transition from a) to b) is jumplike.

the channel (Fig. 3). Let us take the original equation (3)

$$2\rho c_2^2(p_0-p_2)=(p_2-p_1)^2,$$

and let us multiply out and transform, so that

$$p_2^2-2(p_1-\rho c_2^2)p_2+(p_1^2-2\rho c_2^2 p_0)=0.$$

Having solved the quadratic equation and removing ρc_2^2 from under the radical ρc_2^2, we determine p_2:

$$p_2=p_1-\rho c_2^2\pm\rho c_2^2\sqrt{1+\frac{p_0-p_1}{\frac{\rho}{2}c_2^2}}.$$

Since $p_1 = p_s + p_g$ and $c_0 = c_2$, and keeping (5) and (6) in mind, we obtain

$$\frac{(\lambda+2)^2}{K+1}=4. \qquad (7)$$

The test results for variously shaped channels filled with water and kerosene were processed with the dimensionless parameters K and λ, and they are presented in Fig. 4. The curve shows that Eq. (7) makes it possible to determine p_2, i.e., the pressure at the channel outlet at the instant of total flow separation, provided that p_0 and c_2 are known.

When a liquid flows from a wide tube into one that is narrower, the streamlines become distorted at the wall, thus forming local constriction which governs the liquid flow rate for a specified pressure difference. The instant of total flow separation corresponds to a fully defined magnitude of liquid-jet constriction. The coefficient of jet constriction was determined with con-

sideration of the structural features encountered in the test channels in which the ratio between the length of the cylindrical portion at the minimum cross section and the diameter of the orifice was less than 1.5. Thus,

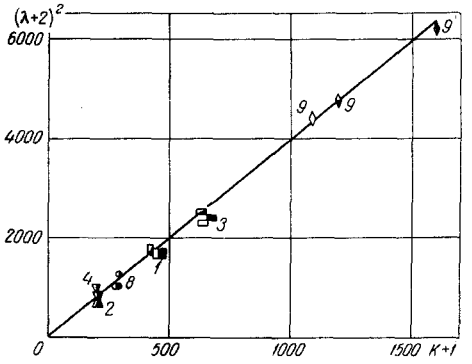

Fig. 4. Experimental relationship $\lambda = f(K)$ in dimensionless coordinates derived for channels of various shapes for water and kerosene at $p_0 = 1.3$ atm abs. Figures show channel numbers. Open symbols refer to water at t = 15° C; filled symbols refer to kerosene at t = 15° C; mixed symbols refer to water at t = 60° C.

on discharge from such nozzles, the liquid does not come into contact with the surface of the cylindrical portion of the orifice, and the jet exhibits a diameter that is smaller than that of the orifice. The cross-sectional area of the jet was calculated from the formula

$$F_{str} = \frac{Q}{\sqrt{\frac{2[p_1^* - (p_s + p_g)]}{\rho}}}.$$

The jet constriction factor was found from the ratio

$$\varphi = \frac{F_{str}}{F_{ori}}.$$

Analysis of the experimental results for water and kerosene—shown in Table 1—demonstrate that the constriction is a function of the inlet shape (see Fig. 1); the smoother the inlet, the larger the coefficient φ. The values of the left-hand member of the equation

$$\frac{p_1^* - (p_s + p_g)}{\frac{\rho}{2} c_1^2} = 1, \qquad (8)$$

given in Table 2, have been calculated without consideration of a jet constriction very much greater than unity. In comparing the cavitational regimes of variously shaped channels, we must therefore take into consideration the actual constriction of the jet.

Table 1

Jet Constriction Factors Derived from Experimental Data for the Case of Liquid Separation Flow

Channel number	φ	Channel number	φ
1	0.915	4	0.72
2	0.72	8	0.62
3	0.7	9	0.56

Impulsive effects result from premature liquid separation from the solid channel surface with a drop in pressure across the outlet, and they promote formation of cavitational rupture within the liquid itself. We studied the strength of various liquids under conditions of impulsive pressures to determine their effect on cavitation processes, and for this purpose we fabricated a plexiglas vessel which we filled with the test liquid. After properly evaporating the vessel, it was subjected to impact loads. The experiment showed that the rupture-resistance of water is a function of the pressure within the vessel, as well as of the impact force. For example, only very weak taps are needed for the rupture of tap water under a pressure close to the vapor pressure of saturated steam, so that bubble collapse becomes visible, and so that the crackling sound that is characteristic of cavitation can be heard. Air is initially released from the liquid in this case in large quantities, and then in decreasingly smaller amounts, as the number of taps increases and as the air is evacuated. Since the cavitation becomes more pronounced as the liberation of the dissolved air diminishes in intensity, all of the air is first removed from the water by evacuating the vessel and shaking it. As the pressure in the vessel rises to 0.6–0.8 atm abs, harder impact is needed for cavitation to result.

Table 2

Similar Discharge Regimes for Variously Shaped Channels Filled with Water and with Kerosene ($p_0 = 1.3$ atm abs)

φ	The left-hand member of (8), without consideration of jet constriction
0.915	1.2
0.72	1.9
0.7	2.0
0.62	2.6
0.56	3.5

A system of standing pressure waves is formed in the case of periodic vibration loads. The rupture of the liquid occurs at certain points within the container in this event. The appearance of cavitation in a liquid following the formation of a standing wave has been studied experimentally. We used a cylindrical plexiglas vessel for this purpose, and provision was made for sensors to fix the jumpwise variations in the electrical conductivity of the medium at the instant that the liquid ruptured at a given point within the vessel. The test was carried out in the following sequence. After positioning the cylindrical vessel vertically and filling it with water, the liquid was degassed by lowering the pressure over its surface and shaking the vessel. The vessel was then subjected to a sharp upward jolt. The vibrations began on closure of the vapor cavity formed when the liquid separated from the bottom of the vessel. The liquid surface was struck by a shock

wave which was immediately reflected in the form of an expansion wave. The interaction of the incident and reflected waves resulted in the formation of a standing wave. At this instant ruptures occurred throughout the entire cross section of the vessel, within a narrow layer of liquid situated in the middle of the liquid column, at the point where the incident and reflected waves met. The test was carried out for various quantities of water within the vessel. The rupture times were noted from signals emitted by electrodes between which current was passed. The time intervals were measured with an oscillograph. Calculation showed that for a vessel with a diameter of 50 mm and a length of 1220 mm, with a liquid-column height of 1040 mm, the time interval τ_1 from impact to the appearance of rupture amounts to 0.0025 sec. With a column height of 690 mm, this interval is $\tau_2 = 0.0017$ sec. In both of the experiments, the pressure-wave velocity—determined from the condition of simultaneity for the appearance of liquid ruptures and the formation of a standing wave within the cylindrical vessel—proved to be equal to 620 m/sec. This result was confirmed by calculation with the formula of Zhukovskii [2].

Thus we established that the onset of cavitation within a liquid may, in addition to ultrasonic vibrations, also be caused by individual impulsive phenomena, as well as by low-frequency vibration on the part of rigid system elements.

NOTATION

p_0^* is the total inlet pressure; p_2^* is the total outlet pressure; p_1^* is the total pressure in the liquid stream, p_0 is the static inlet pressure; p_2 is the static outlet pressure; p_1 is the static pressure in the stream; c_0 is the inlet flow velocity; c_2 is the outlet flow velocity; c_1 is the stream velocity; ρ is the liquid density; p_S is the vapor pressure of the saturated steam; p_g is the partial pressure of gas in the cavity; Q is the fluid flow rate; F is the area of the channel cross section; φ is the stream constriction factor; τ is the time.

REFERENCES

1. P. Eisenberg and M. P. Tulin, Cavitation, in: Handbook of Fluid Dynamics, McGraw-Hill, N. Y., 1961.

2. N. E. Zhukovskii, Collected Works, Vols. 2, 3 [in Russian], 1948.

17 May 1967